

Article

Biometric and Eddy Covariance Methods for Examining the Carbon Balance of a *Larix principis-rupprechtii* Forest in the Qinling Mountains, China

Jie Yuan ¹ , Shibu Jose ², Zhaoyong Hu ¹, Junzhu Pang ^{1,3}, Lin Hou ^{1,3} and Shuoxin Zhang ^{1,3,*}

¹ College of Forestry, Northwest A&F University, Xianyang 712100, China; yuanjie@nwsuaf.edu.cn (J.Y.); huzy418@gmail.com (Z.H.); pangjunzhu@nwsuaf.edu.cn (J.P.); houlin1969@163.com (L.H.)

² School of Natural Resources, University of Missouri, Columbia, MO 65211, USA; joses@missouri.edu

³ Qinling National Forest Ecosystem Research Station, Huoditang, Ningshan 711600, China

* Correspondence: sxzhang@nwsuaf.edu.cn; Tel./Fax: +86-29-8708-2993

Received: 20 December 2017; Accepted: 25 January 2018; Published: 29 January 2018

Abstract: The carbon balance of forests is controlled by many component processes of carbon acquisition and carbon loss and depends on the age of vegetation, soils, species composition, and the local climate. Thus, examining the carbon balance of different forests around the world is necessary to understand the global carbon balance. Nevertheless, the available information on the carbon balance of *Larix principis-rupprechtii* forests in the Qinling Mountains remains considerably limited. We provide the first set of results (2010–2013) from a long-term project measuring forest-atmosphere exchanges of CO₂ at the Qinling National Forest Ecosystem Research Station (QNFERS), and compare the net ecosystem exchange (NEE) based on biometric measurements with those observed via the eddy covariance method. We also compare the total ecosystem respiration via scaled-up chamber and eddy covariance measurements. The net primary productivity (NPP) was $817.16 \pm 81.48 \text{ g}\cdot\text{C}\cdot\text{m}^{-2}\cdot\text{y}^{-1}$, of which ΔB_{living} and D_{total} accounted for 77.7%, and 22.3%, respectively. Total ecosystem respiration was $814.47 \pm 64.22 \text{ g}\cdot\text{C}\cdot\text{m}^{-2}\cdot\text{y}^{-1}$, and cumulative annual soil respiration, coarse woody debris respiration, stem respiration, and leaf respiration were 715.47 ± 28.48 , 15.41 ± 1.72 , 35.28 ± 4.78 , and $48.31 \pm 5.24 \text{ g}\cdot\text{C}\cdot\text{m}^{-2}\cdot\text{y}^{-1}$, respectively, accounting for 87.85%, 1.89%, 4.33%, and 5.93% of the total ecosystem respiration. A comparison between ecosystem respiration from chamber measurements and that from eddy covariance measurements showed a strong linear correlation between the two methods ($R^2 = 0.93$). The NEE of CO₂ between forests and the atmosphere measured by eddy covariance was $-288.33 \pm 25.26 \text{ g}\cdot\text{C}\cdot\text{m}^{-2}\cdot\text{y}^{-1}$, which revealed a carbon sink in the *L. principis-rupprechtii* forest. This number was 14% higher than the result from the biometric measurements ($-336.71 \pm 25.15 \text{ g}\cdot\text{C}\cdot\text{m}^{-2}\cdot\text{y}^{-1}$). The study findings provided a cross-validation of the CO₂ exchange measured via biometric and eddy covariance, which are beneficial for obtaining the true ecosystem fluxes, and more accurately evaluating carbon budgets.

Keywords: carbon balance; Qinling Mountains; biomass regression model; eddy covariance; net primary productivity; net ecosystem exchange

1. Introduction

Forests play a critical role in the global carbon cycle [1,2], and since the 1990s, substantial data have been acquired to clarify the contributions of forest ecosystems to the global carbon cycle [3–5]. The Qinling Mountains in central China provide an important climate boundary between the southern subtropics and the northern temperate zone, where the typical vegetation of both climate zones is present together with astonishingly high biodiversity [6]. Nevertheless, information relevant to the carbon balance from forests in the Qinling Mountains remains considerably limited. Studies have

demonstrated that mountain forests are 'hot spots' for carbon cycling and are expected to be more strongly affected by climate change than lowland forests due to their sensitivity to warming [7,8]. Therefore, there is an urgent need for increased knowledge about the carbon fluxes in various mountain forests, especially those in the Qinling Mountains.

Larix principis-rupprechtii is adapted to high light levels and can tolerate freezing temperatures. This species grows in deep, well-drained acidic or neutral soils and is a valuable reforestation species in China that is distributed over ten provinces. Due to its rapid growth, high-quality wood, resistance to adverse climate and soil conditions, and high wind resistance, the tree is used for forest regeneration and afforestation of barren hills. *L. principis-rupprechtii* forests in the Qinling Mountains serve as major research sites for forest ecosystem studies because they represent the regional vegetation in the temperate coniferous forest domain of China and are also a major component of temperate forests globally. In addition, the *L. principis-rupprechtii* forest is sensitive to global change [9]. In the Qinling Mountains, from 1958 to 1986, the area afforested with *Larix* reached 0.3×10^4 ha [10]. Although Zhou et al. estimated the carbon budget of a *Larix* forest in China [11], there is still considerable uncertainty about the strength of the carbon source/sink in this forest due to discrepancies in estimation methods and variations in age, management, and climate [12,13]. Thus, to accurately determine the carbon balance of *Larix* forests, an adequate understanding of the processes that control net CO₂ exchange in a young *L. principis-rupprechtii* planted forest in the temperate regions is required.

The carbon balance at the ecosystem level (net ecosystem exchange, NEE) is controlled by many component processes of carbon acquisition (photosynthesis, tree growth, forest ageing, and carbon accumulation in soils) and carbon loss (respiration of living biomass, tree mortality, microbial decomposition of litter, oxidation of soil carbon, degradation, and disturbance) [14]. However, previous studies have suggested respiration as the main determinant in controlling the carbon balance of ecosystems [13]. Ecosystem respiration is composed of autotrophic and heterotrophic components, whose contributions to total respiration vary in space and time. Components of respiration include soil (roots and microorganisms), coarse woody debris (CWD), and stem and leaf respiration, which are controlled by the complex interaction of many factors, including temperature, moisture, canopy cover, stand age, and nutrient contents [4,15]. Few studies have investigated the seasonal and annual variability of these respiratory components in detail [4,16]. Hence, it is absolutely necessary to quantify the ecosystem's respiratory components, which can allow researchers to determine the contribution of each component flux to the overall ecosystem respiration and improve our understanding of ecosystem respiration dynamics [17].

Currently, the foremost techniques for measuring NEE are the eddy covariance technique and the biometric technique. Each technique has advantages and disadvantages. The eddy covariance method is a micrometeorological technique and has been widely used in different ecosystems [18,19]. The eddy covariance technique has numerous advantages: (1) it is nondestructive and has a low workload, (2) it provides observations at the ecosystem scale, and (3) it yields continuous records that address time scales every half hour to the length of the data record [16,20]. Since the early 1990s, more than 500 eddy covariance flux towers have been built in numerous ecosystems around the world [21]. However, there are still deficiencies in the eddy covariance method. Firstly, the measurements become unreliable or unavailable when the atmospheric conditions (wind, temperature, humidity, CO₂) are unsteady, the terrain is uneven, or there is very weak turbulence, as sometimes occurs at night [22,23]. Secondly, this method is valid for usage on large-scale field plots and cannot provide information on the component carbon fluxes [16]. The biometric method offers the advantages of lower cost and simplicity, in principle. Moreover, the chambers are portable and well suited for small-scale studies, which is appropriate for replicated measurements in multiple small plots of field trials and is also necessary for estimating the contributions of component carbon fluxes (for example, net primary production (NPP), heterotrophic respiration, and autotrophic respiration) to the total fluxes. However, some drawbacks have limited the application of the biometric method for NEE measurements. For example, (1) a variety of potential errors, such as modifications in the enclosed microclimate, pressure artefacts, and spatial

heterogeneity, may occur [24]; (2) it cannot effectively sample the full spatial variation of patch-specific fluxes; (3) it cannot observe the full short-term (intra-daily) and intermediate (inter-daily) temporal variations that occur within a site; and (4) large uncertainties in scaled-up estimates may result in over- or underestimates of the actual fluxes [25].

In short, both the eddy covariance and the biometric methods must be inaccurate in measuring NEE due to the weaknesses associated with using either method alone. Few studies have conducted comparisons of eddy covariance and biometric-based measurements of NEE, especially relative to measurements taken simultaneously at the same site using the two different methods [26]. Thus, comparing the NEE measured using the eddy covariance and the biometric methods is necessary to highlight the potential sources of errors. Such a comparison is straightforward but requires a strict methodology for testing the accuracy and consistency of the eddy covariance and the biometric fluxes.

This paper presents the first set of results (2010–2013) from a long-term project measuring forest-atmosphere exchanges of CO₂ using the eddy covariance and biometric methods in a *L. principis-rupprechtii* forest in the Qinling Mountains. The objectives of our study were as follows: (1) to describe measurements of soil, coarse woody debris (CWD), stem, and leaf respiration based on chamber methods and to combine these measured fluxes with continuous measurements of temperature to model the respiration of each ecosystem component; (2) to estimate the spatial and temporal variability of ecosystem respiration and the percentage of the total ecosystem respiration of each component based on chamber measurements; and (3) to compare the total ecosystem respiration based on scaled-up chamber measurements and NEE based on biometric measurements with those observed via the eddy covariance method and to evaluate the carbon balance of the *L. principis-rupprechtii* forest at this site.

2. Materials and Methods

2.1. Study Area

The study area for the ecosystem component measurements covered 1 ha centered on a tower equipped for eddy covariance measurements of carbon dioxide exchange located at the Huoditang Experimental Forest Farm of Northwest A&F University in the Qinling Mountains, Shaanxi Province, China (Figure S1). The altitude is 2150 m, and the geographic coordinates are 33°27'42" N latitude and 108°28'54" E longitude. The annual average temperature is 10.80 °C, the annual precipitation 1200 mm, and the climate belongs to the temperate zone. The period of snow cover is from December to March, with a maximum depth of approximately 20 cm. The soil is classified as mountain brown earth.

The study area was selectively logged in the 1960s and 1970s, and since then, there have been no major anthropogenic disturbances except for small amounts of illegal logging. Since the natural forest protection project was initiated in 1998, human activities have almost vanished in the region. To reduce disturbance, the permanent plot was protected by an enclosure. The site is level (a mean slope of 5°), which is ideal for this study, and the overstory and understory of the forest are homogeneous. Moreover, the results of the data quality estimate (footprint analysis, energy balance estimate, eddy statistic estimate, and power spectrum estimate) implied that not only the location selected but also the configuration of this observational system are comparable for observations of the fluxes in the long run [27].

The forest used for the current research was 50 years old and was dominated by *L. principis-rupprechtii*. The mean stand height, diameter at breast height (DBH), and stand density were 16 m, 18 cm, and 1585 trees·ha⁻¹, respectively. In the shrub layer, the height varied from 80 cm to 520 cm and the percent cover was 28%. The major shrubs species present were *Euonymus phellomanus*, *Lonicera hispida*, *Lindera glauca*, and *Rubus pungens*, together with herbs such as *Carex leucochlora*, *Deyeuxia arundinacea*, *Lysimachia christinae*, *Thalictrum minus*, *Anaphalis aureopunctata*, *Dioscorea nipponica*, *Rubia cordifolia*, and *Sinacalia tangutica*, and the fern *Dryopteris goeringiana*. The average height of the herbs was 60 cm, and the percent cover was 40%.

2.2. Biometric Measurements

2.2.1. Plot Measurements

In summer 2009, we established a permanent plot in the *L. principis-rupprechtii* forest. The 1 ha plot was divided into 25 quadrats 20 m × 20 m in size. The quadrats were each subdivided into 16 sub-quadrats 5 m × 5 m in size. A total of 1585 trees and 2728 shrubs in these sub-quadrats were permanently marked with aluminum labels and numbered consecutively. Based on the plot investigation, 10 standard trees outside the plot were felled. The leaves and branches at different canopy positions and orientations and the stems of different diameters were all collected, and the roots were dug up from the 10 standard trees to measure the carbon content ratio and evaluate the biomass. The DBH of all trees (including dead and new trees) were documented in August of each year during 2009–2013 to estimate (the annual change in) the biomass, which was calculated via the regression model developed in a previous study in this region (Table S2) [28].

We also documented the species, height, crown width, and basal stem diameter of all shrubs (including dead and new shrubs) in August of each year during 2009–2013 for biomass calculations. Based on the species present within the plots, *E. phellomanus*, *L. hispida*, *L. glauca*, and *R. pungens* outside the plot were dug up, with totals of 55, 48, 78, and 62 individual plants, respectively. The species, height, crown width, and basal stem diameter of these harvested shrubs were recorded, and they were then taken back to the laboratory to measure the carbon content ratio and develop a biomass regression model (Table S3).

To reduce disturbance, based on the plot investigation, we selected twenty 1 m × 1 m groundcover quadrats outside the plot in August of 2009–2013. All of the herbs were dug out in the twenty quadrats each year in order to measure the carbon content ratio and biomass. The twenty quadrats were not repeated each year, and new quadrats were selected each year.

In order to accurately estimate the root biomass and correct the fine root loss caused by digging, we used soil coring to supplement the fine root biomass [29]. A representative root sample was extracted from soil cores of 30 cm in length and 1.8 cm in diameter (76 cm³). We selected twenty soil cores outside the plot in August of 2009–2013. All soil cores were extracted each year to supplement the fine root biomass. The twenty soil cores were not repeated each year, and new soil cores were selected each year. Litterfall was collected from the beginning of August 2009 to August 2013 at monthly intervals. Twenty 1 m × 1 m litter traps were randomly erected in the plot. Each trap consisted of 2 mm mesh nylon netting (on a wooden frame) suspended from a wire hoop and held 30 cm above the ground by four metal poles.

2.2.2. Carbon Content Ratio

The samples of trees, shrubs, and herbs were classified into species and organs (stem, bark, branch, leaf, and root), and the stems, branches, and roots were cut into 10 cm lengths. In each species, the same organs of the samples were pooled into one composite sample, while the twenty litterfall traps were also pooled into one composite sample. These composite samples were dried at 85 °C to constant weight (approximately 72 h) and then crushed to pass through a No. 200 mesh (0.074 mm) in order to measure the carbon content ratio. Each composite sample was repeatedly measured three times with a TOC analyzer (TOC-VTH-2000A, Shimadzu, Japan), and the average value was obtained for the carbon content ratio of litterfall and the different organs of the trees, shrubs, and herbs.

2.2.3. Net Primary Productivity (NPP)

Forest NPP estimates have been based primarily upon measurements of stems, bark, branches, and roots (including coarse and fine roots) biomass gain using regression models for trees and shrubs and harvest methods for other ecosystem components (herbs and litterfall). NPP was estimated using the following equations:

$$\text{NPP} = \Delta B_{\text{living}} + D_{\text{total}} \quad (1)$$

$$\Delta B_{\text{living}} = \sum T_i O_i + \sum S_j O_j + \sum H_r O_r \quad (2)$$

$$D_{\text{total}} = \sum D_{ti} O_i + \sum D_{sj} O_j + L \times P \quad (3)$$

where ΔB_{living} is the increment in live plant biomass, T_i is the live tree biomass increment of the i th organ (except for leaf), O_i is the tree carbon content ratio of the i th organ, S_j is the live shrub biomass increment of the j th organ (except for leaf), O_j is the shrub carbon content ratio of the j th organ, H_r is the herbaceous biomass increment of the root, O_r is the herbaceous carbon content ratio of the root, D_{total} is the sum of dead plant mass, D_{ti} is the dead tree mass of the i th organ (except for leaf), O_i is the tree carbon content ratio of the i th organ, D_{sj} is the dead shrub mass of the j th organ (except for leaf), O_j is the shrub carbon content ratio of the j th organ, L is the mass of litterfall, and P is the carbon content ratio of litterfall. Herbivore loss is often assumed to be negligible in healthy stands [30] and was not estimated in this study.

2.2.4. Leaf Area Index

The LAI-2000 plant canopy analyzer (LI-COR, Inc., Lincoln, NE, USA) is designed to estimate the leaf area index (LAI) of plant canopies indirectly from measurements of radiation above and below the canopy based on a theoretical relationship between leaf area and canopy transmittance [31]. The below-canopy measurements were made at 40 points, which were marked with red stakes and located along permanent transects; the sampling distance was 15 m in this forest. Above-canopy measurements were taken automatically every 15 s by a second instrument in the center of an open field situated nearby. The fish-eye lens of the instrument was covered by a view cap with a 90° opening to ensure that the reference measurements were not influenced by the trees surrounding the clearings or by the operator [32]. In taking canopy measurements, the sensor was held so that the same portion of the sky and the same level (between 1 and 1.5 m above ground) was occluded for both sensors (above- and below-canopy measurements). The LAI measurements were made every 2 weeks from April to November in 2010–2013.

2.2.5. Micrometeorological Measurements

A full suite of micrometeorological measurements was taken from the weather station located 20 m away from the plot, including air temperature and humidity (HMP45C, Vaisala, Helsinki, Finland), photosynthetically active radiation, soil temperature (10 cm), and precipitation. Data from all the sensors were recorded on data loggers (CR-1000, Campbell Scientific, Logan, UT, USA), and the data were downloaded every 2 weeks to a laptop personal computer (PC).

2.2.6. Soil Respiration

Soil respiration was measured using an LI-6400-09 soil chamber connected to an LI-6400 portable photosynthesis system (LI-COR, Inc., Lincoln, NE, USA). Thirty soil collars, each with a height of 10 cm and a diameter of 10 cm, were randomly placed in the 1 ha plot. To avoid influence on the measurement of soil respiration, the soil collars were inserted into the soil at the depth of 2 cm one week before the measurement of soil respiration. The surface vegetation inside the soil collars was cleared 1 day before the measurement, and the topsoil was kept intact to avoid its influence on the measured results. Surface efflux was measured three times in succession for each collar during each measurement period. Soil temperature at 10 cm was measured adjacent to each respiration collar with a portable temperature probe provided with the LI-6400. The measurements were made every 2 weeks from April to November in 2010–2013.

We used an exponential equation to analyze the relationship between respiration and temperature:

$$R = R_0 e^{\beta T} \quad (4)$$

where R is the component respiration (soil ($\mu\text{mol}\cdot\text{m}^{-2}\cdot\text{s}^{-1}$), root ($\mu\text{mol}\cdot\text{m}^{-2}\cdot\text{s}^{-1}$), coarse woody debris ($\mu\text{mol}\cdot\text{m}^{-3}\cdot\text{s}^{-1}$), stem ($\mu\text{mol}\cdot\text{m}^{-3}\cdot\text{s}^{-1}$), or leaf ($\mu\text{mol}\cdot\text{g}^{-1}\cdot\text{d}^{-1}$)); T is the temperature of each component ($^{\circ}\text{C}$); and R_0 and β are fitted parameters. The temperature dependence of respiration is often described by the Q_{10} value, which is called the temperature sensitivity of respiration. The respiration parameter, Q_{10} , can be derived from $Q_{10} = \exp(10\beta)$. Estimated parameters were used to predict the soil respiration for every 0.5 h over 4 years based on continuous temperature measurements from the weather station.

2.2.7. Root Respiration

The trenching method was used to estimate the root respiration [33]. The trenched plot (20 m \times 20 m) was established adjacent to the permanent plot at this site. We also randomly established twenty 50 cm \times 50 cm subplots in the trenched plot in August 2009. Each subplot was prepared by making vertical cuts along the boundaries to 50 cm below the ground surface (approximately the bottom of the root zone) with a steel knife, severing all roots. The roots were removed, and fiberglass sheets were installed to prevent roots from entering. The trenches were backfilled with the same soil. The aboveground parts of all plants growing in the subplots were cut off, and new seedlings and re-growth from the roots were periodically clipped when necessary.

Twenty soil collars, each with a height of 10 cm and a diameter of 10 cm, were inserted into the soil in the subplots. The soil respiration in the trenched plot was measured using the same method for soil respiration.

We used the following equation to calculate the root respiration (R_R , $\mu\text{mol}\cdot\text{m}^{-2}\cdot\text{s}^{-1}$):

$$R_R = R_S - R_C \quad (5)$$

where R_S is the soil respiration in the permanent plot ($\mu\text{mol}\cdot\text{m}^{-2}\cdot\text{s}^{-1}$) and R_C is the soil respiration in the trenched plot ($\mu\text{mol}\cdot\text{m}^{-2}\cdot\text{s}^{-1}$).

2.2.8. Coarse Woody Debris Respiration

We used the standard method developed by the United States Department of Agriculture (USDA) Forest Service and the Long Term Ecological Research (LTER) programme to define woody debris as CWD, which was further categorized into logs, snags, and stumps [34]. The downed or leaning deadwood with a diameter at the widest point ≥ 10 cm and length ≥ 1 m were included in the group. The dead trees with a gradient (departure from vertical direction) $\leq 45^{\circ}$ were considered as snags, while those with a gradient $> 45^{\circ}$ were classified as logs. The vertical deadwood with a height ≤ 1 m was considered as stumps. Each piece of CWD was assigned to one of five decay classes on the basis of differences in internal and external tissue characteristics (Table S4) [35]. The numbers 1, 2, 3, 4, and 5 represent different decomposition stages, i.e., 1 represents the initial stage and 5 represents the final stage.

CWD respiration was measured for the five decay classes in the plot. Three pieces of CWD were sampled for CWD respiration in each decay class, and three fixed plates were mounted on each low decay class of CWD (sufficient sound wood was present) with silicon sealant at a random azimuth. A custom Plexiglas cuvette, 800 cm³ in volume with an 80 cm² opening, was closely attached to the mounting plate just before each measurement. CWD respiration was measured three times in succession for each cuvette during each measurement and three times during the day at each cuvette. CWD temperature at 10 cm deep was measured adjacent to each cuvette with a portable temperature probe provided with the LI-6400. For the more advanced decay classes, these CWD samples were placed into the containers to measure. The measurements were made every 2 weeks from April to November in 2010–2013.

The measured CWD respiration rates per unit area were converted to rates per unit volume. We used the exponential function (Q_{10} function) to analyze the response of CWD respiration per unit

of volume to CWD temperature (Equation (4)). Continuous CWD temperatures were calculated by the model, which simulated the relationship between CWD temperatures and 10 cm soil temperatures (Figure S5).

To upscale the chamber measurements of CWD respiration to the stand level, we calculated the volume of the five decay classes of CWD in the plot. Forest censuses were conducted in August of each year during 2009–2013 to determine the CWD volume. Each log or stump was considered as a cylinder; consequently, we used Smalian's formula to produce a volume estimate through the length and cross-sectional areas at the basal and distal ends of the cylinder [36]. For snags, we used the height and diameter in a species-specific wood volume equation, thus calculating the volume of each piece of the snag.

2.2.9. Stem Respiration

Fifty fixed plates were mounted on the trunks of 50 standard trees with silicon sealant at approximately 130 cm in height and a random azimuth. We used the same cuvette that was used to measure CWD respiration for measuring stem respiration; the cuvette was closely attached to the mounting plate just before each measurement. For the CWD respiration measurements, stem respiration rates were measured three times in succession for each cuvette during each measurement and three times during the day at each cuvette. The measurements were made every 2 weeks with an LI-6400 portable photosynthesis system (LI-COR, Inc., Lincoln, NE, USA) from April to November in 2010–2013. Stem temperature was measured with a portable temperature probe provided with the LI-6400 inserted into the sapwood near the cuvette of each sample tree. The sapwood thickness and wood mass density of each standard tree were measured from tree cores.

Measured stem respiration rates per unit area were converted to rates per unit of sapwood volume based on sapwood area and tree DBH, assuming a wedge-shape volume had contributed to the respiration rates. We used the exponential function (Q_{10} function) to analyze the response of stem respiration per unit of sapwood volume to stem temperature (Equation (4)). Continuous stem temperatures were calculated by the model, which simulated the relationship between stem temperatures and air temperatures (Figure S6).

To upscale the chamber measurements of stem respiration to the stand level, we estimated the total sapwood volume per unit of ground area in the plot. We assumed that branch respiration per volume had the same rate as stem (bole) respiration, similar to the assumptions made by Law et al. [37], Xu et al. [38], and Bolstad et al. [4].

After measuring the DBH and sapwood thickness, we estimated the sapwood volume of 30 sample trees to develop the regression model for sapwood volume:

$$\ln V_p = 0.90589 \ln (D^2H) - 10.31542 \quad (6)$$

where V_p is the sapwood volume including that from stems and branches (m^3), D is the DBH (m), H is the tree height (m), and the correlation coefficient is 0.9452. Equation (6) was used to estimate the sapwood volume of the whole stand and the average sapwood volume per ground area.

2.2.10. Leaf Respiration

Leaf respiration was measured from 30 leaves collected from 10 *L. principis-rupprechtii* trees, 30 leaves from shrubs, and 30 leaves from herbs from April to November in 2010–2013. Following the method of Bolstad et al. [4], branches from species from random heights and directions in the canopy were detached at night and immediately placed in a plastic bag with a moistened paper towel and transported in the dark to a nearby laboratory. Fully expanded leaves were detached just before measurement. All measurements were made within 3 h of branch harvest. Leaf respiration rates were measured from 5 to 25 °C with a controlled temperature LI-6400 portable photosynthesis system (LI-COR, Inc., Lincoln, NE, USA). Leaf area was measured with an AM-300 portable leaf area meter

(ADC Bioscientific Limited, SG12, 9TA, Cambridge, UK). Leaves were oven dried at 65 °C and weighed. The measured leaf respiration rates per unit area were converted to rates per unit of dry biomass.

We used the exponential equation (Equation (4)) to fit the leaf respiration per unit of dry biomass as a function of leaf temperature for each species. We assumed in this study that the leaf temperature was the air temperature.

To upscale chamber measurements of leaf respiration to the stand level, we estimated the total leaf dry biomass per unit of ground area in the plot. The dry leaf biomass of shrubs and herbs was estimated by our study, while the dry leaf biomass of *L. principis-rupprechtii* was estimated by the regression model based on a previous study in this region [28].

2.2.11. Net Ecosystem Exchange

The annual net ecosystem exchange of CO₂ (NEE, g·C·m⁻²·y⁻¹) can be estimated using the following equation according to the measured annual rates of component respirations and net primary production (NPP):

$$NEE = R_S + R_{CWD} - R_R - NPP \quad (7)$$

where R_S is the soil respiration (g·C·m⁻²·y⁻¹), R_{CWD} is the CWD respiration (g·C·m⁻²·y⁻¹), Equation (5) was used to calculate the R_R (g·C·m⁻²·y⁻¹), and Equation (1) was used to calculate the NPP (g·C·m⁻²·y⁻¹).

2.3. Eddy Covariance Measurements

To compare with biometric measurements, fluxes of CO₂ were measured from a tower at 30 m above ground in the *center* of the stand. A three-dimensional sonic anemometer (CSAT-3, Campbell Scientific, Inc., Logan, UT) and an open-path infrared gas analyzer (LI-7500, LI-COR, Lincoln, NE, USA) mounted at a height of 25 m measured the three components of the wind velocity vector, sonic temperature, and the densities of water vapor and CO₂. These components were sampled at 10 Hz by a data logger (CR-5000, Campbell Scientific, Logan, UT, USA), which also calculated the 30 min covariance using Reynolds block averaging. Surface fluxes were later calculated off-line after performing a two-dimensional coordinate rotation and accounting for density fluctuations [39]. NEE data were screened for weak turbulence friction velocity at night. Although we found only a negligible trend of increasing NEE with u^* , we calculated an annual NEE using a u^* threshold of 0.15 m·s⁻¹. To fill the gaps, a double-directional interpolation model of artificial neural networks (ANNs) was used [27]. Nighttime NEE was assumed to be a measurement of ecosystem respiration and was extrapolated to all times by using a temperature response function as described by Cook et al. [40] and Desai et al. [41].

2.4. Statistical Analyses

One-way ANOVAs were used to determine the effect of the 10 cm soil temperature on the soil respiration, of CWD temperature on the respiration of different CWD decay classes, of sapwood temperature on the stem respiration, and of air temperature on the leaf respiration. An exponential equation was used to simulate the relationship between respiration and temperature. The relationship between the CWD temperature and the 10 cm soil temperature was simulated using a regression model. A regression model was also used to simulate the relationship between sapwood temperature and air temperature. The sapwood volume was estimated by a regression model. Moreover, the eddy covariance technique and chamber-based estimates were simulated based on a linear model. All statistical analyses were conducted using the SAS 8.0 Statistical Package, with a *p*-value of 0.05 set as the limit for statistical significance. Origin 8.0 (OriginLab Corporation, Northampton, MA, USA) was used to draw the graphs.

3. Results

3.1. Environmental Factors

There was a clear seasonal pattern in air temperature and 10 cm soil temperature during 2010–2013 (Figure S7). The air temperature changed more dramatically, but the variation of the 10 cm soil temperature was consistent with the air temperature. The annual mean air temperature was 10.82 ± 9.66 , 10.94 ± 9.78 , 10.59 ± 9.60 , and 10.89 ± 9.84 °C for 2010 to 2013, respectively. The annual mean 10 cm soil temperature was 11.12 ± 8.09 , 11.22 ± 8.19 , 10.93 ± 8.04 , and 11.18 ± 8.24 °C for 2010 to 2013, respectively. Due to rain, the photosynthetic active radiation was relatively low from June to August for all years (Figure S8). The annual mean photosynthetically active radiation was 147.81 ± 92.09 , 149.05 ± 103.63 , 146.19 ± 94.49 , and 144.54 ± 81.05 $\mu\text{mol}\cdot\text{m}^{-2}\cdot\text{s}^{-1}$ for 2010 to 2013, respectively.

3.2. Soil Respiration

There was a significant exponential relationship between soil respiration and the 10 cm soil temperature. The parameters in Equation (4) for soil respiration are summarized in Table 1. Equation (4) allows us to estimate the year-round soil respiration using the 10 cm soil temperature as an independent variable. There was an obvious seasonal pattern of soil respiration in 2010–2013 (Figure 1). Soil respiration includes soil heterotrophic respiration, root respiration, and litter respiration; root respiration accounted for $35\% \pm 7\%$ of the soil respiration on average in 2010–2013 (Figure 1). The total soil respiration was 710.37 ± 20.14 , 721.45 ± 22.45 , 692.77 ± 19.64 , and 737.27 ± 24.27 $\text{g}\cdot\text{C}\cdot\text{m}^{-2}\cdot\text{y}^{-1}$ for 2010 to 2013, respectively. The lower soil respiration in 2012 was consistent with the soil temperature in 2012, which was lower than in other years.

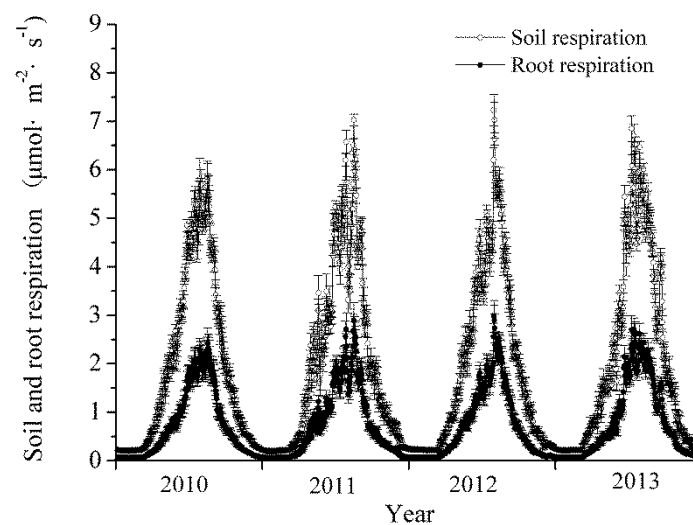


Figure 1. Daily mean soil and root respiration in the *L. principis-rupprechtii* forest during 2010–2013. Error bars are based on 0.5 h soil temperatures as experimental unit ($n = 48$).

Table 1. Parameters in the temperature response function (Equation (4)) for soil respiration (R_S , $\mu\text{mol}\cdot\text{m}^{-2}\cdot\text{s}^{-1}$), root respiration (R_R , $\mu\text{mol}\cdot\text{m}^{-2}\cdot\text{s}^{-1}$), coarse woody debris (CWD) respiration (R_{CWD} , $\mu\text{mol}\cdot\text{m}^{-3}\cdot\text{s}^{-1}$), stem respiration (R_T , $\mu\text{mol}\cdot\text{m}^{-3}\cdot\text{s}^{-1}$), and leaf respiration (R_L , $\mu\text{mol}\cdot\text{g}^{-1}\cdot\text{d}^{-1}$).

Respiration (R)	R_0	β	Q_{10}	Coefficient of Determination (R^2)	Samples (n)	
R_S	0.22	0.14	4.19	0.76	5760	
R_R	0.12	0.11	3.00	0.66	3840	
R_{CWD}	1	1.03	0.12	3.44	0.72	576
	2	1.30	0.10	2.62	0.81	576
	3	3.25	0.07	2.06	0.73	576
	4	3.43	0.10	2.81	0.76	576
	5	3.03	0.10	2.59	0.82	576
R_T	1.42	0.09	2.51	0.72	9600	
R_L	Tree	3.52	0.07	1.98	0.65	1920
	Shrub	4.81	0.06	1.85	0.68	1920
	Herb	2.75	0.07	1.92	0.65	1920

3.3. Coarse Woody Debris (CWD) Respiration

There was a strong exponential correlation between the respiration of different CWD decay classes and temperature (Table 1). To estimate continuous CWD respiration in the *L. principis-rupprechtii* forest during 2010–2013, we calculated continuous CWD temperature using the model that simulated the relationship between the CWD temperature and the 10 cm soil temperature. The seasonal variation of the CWD respiration per volume indicated that the CWD respiration peaked in July and then followed a decreasing trend with time (Figure 2). We found significant differences in the CWD respiration among the different decay classes in 2010–2013. The maximum respiration across the four years, with a mean of $15.33 \pm 1.32 \mu\text{mol}\cdot\text{m}^{-3}\cdot\text{s}^{-1}$, appeared in decay class 4, which was more than 3 times higher than the minimum in decay class 1 ($4.65 \pm 0.37 \mu\text{mol}\cdot\text{m}^{-3}\cdot\text{s}^{-1}$). Over time, the volume of different CWD decay classes increased (Table 2). The respiration of different CWD decay classes per unit ground area also increased over time, except for a slight decrease in 2012 (Table 2), which was consistent with the temperature of different CWD decay classes.

Table 2. Volume ($\text{m}^3\cdot\text{ha}^{-1}$) and the respiration of different coarse woody debris (CWD) decay classes per ground area ($\text{g}\cdot\text{C}\cdot\text{m}^{-2}\cdot\text{y}^{-1}$) during 2010–2013.

CWD Decay Classes		Year			
		2010	2011	2012	2013
1	Volume	16.83 (1.23)	17.90 (1.51)	18.17 (1.31)	19.21 (1.62)
	Respiration	2.85 (0.23)	3.06 (0.18)	3.02 (0.26)	3.31 (0.28)
2	Volume	14.64 (1.18)	14.90 (1.22)	15.89 (1.08)	16.41 (1.33)
	Respiration	3.03 (0.17)	3.12 (0.25)	3.21 (0.23)	3.49 (0.27)
3	Volume	8.95 (0.82)	9.28 (0.78)	9.40 (0.68)	9.82 (0.72)
	Respiration	2.84 (0.23)	2.97 (0.18)	2.94 (0.23)	3.16 (0.22)
4	Volume	6.39 (0.51)	6.63 (0.48)	6.71 (0.53)	7.03 (0.38)
	Respiration	3.69 (0.19)	3.88 (0.26)	3.80 (0.31)	4.16 (0.34)
5	Volume	5.11 (0.31)	5.30 (0.28)	5.38 (0.38)	5.65 (0.27)
	Respiration	2.16 (0.16)	2.27 (0.21)	2.23 (0.27)	2.44 (0.26)
Total	Volume	51.92 (3.86)	54.01 (4.51)	55.55 (4.39)	58.12 (4.88)
	Respiration	14.57 (1.58)	15.30 (1.35)	15.20 (1.61)	16.56 (1.48)

Note: standard error is provided in brackets.

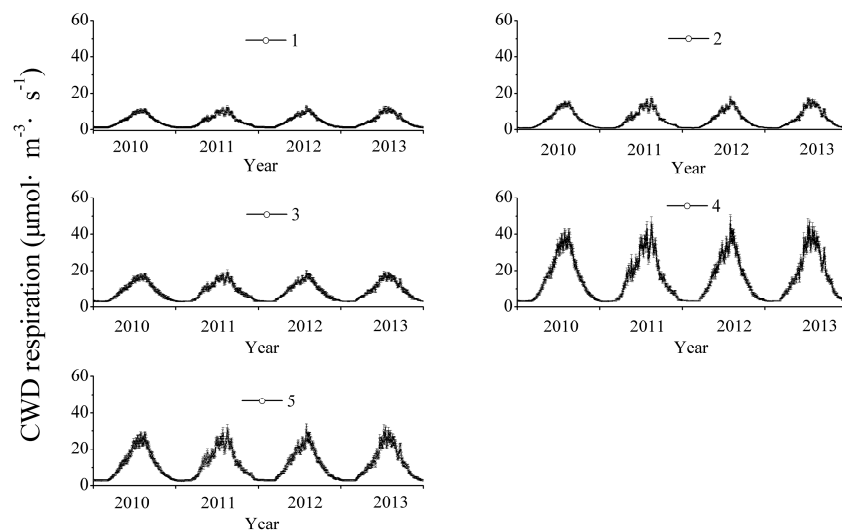


Figure 2. The daily mean respiration of different coarse woody debris (CWD) decay classes in the *L. principis-rupprechtii* forest during 2010–2013. Error bars are based on 0.5 h soil temperatures as experimental unit ($n = 48$).

3.4. Stem Respiration

We found an exponential relationship between stem respiration and sapwood temperature, and the parameters are summarized in Table 1. Because sapwood temperature was not recorded for the whole year, we developed a correlation between sapwood temperature (y) and air temperature (x) ($y = 0.62385 + 0.88813x$, $R^2 = 0.98674$, $n = 108$, $p < 0.0001$). Stem respiration varied seasonally, with the lowest rate in February and the highest in July (Figure 3). Sapwood volume was 189.21 ± 12.31 , 193.52 ± 11.08 , 196.28 ± 15.57 , and 215.21 ± 18.11 $\text{m}^3 \cdot \text{ha}^{-1}$ during 2010 to 2013, respectively. We estimated the stem respiration per unit of ground area as 33.52 ± 2.86 , 34.68 ± 3.18 , 34.12 ± 2.17 , and 38.82 ± 3.22 $\text{g} \cdot \text{C} \cdot \text{m}^{-2} \cdot \text{y}^{-1}$ from 2010 to 2013, respectively.

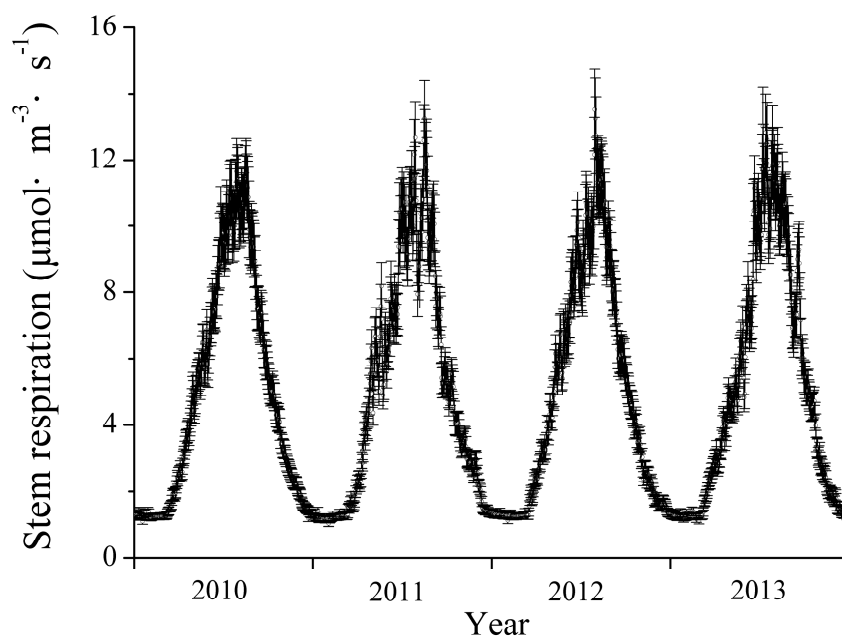


Figure 3. Daily mean stem respiration in the *L. principis-rupprechtii* forest during 2010–2013. Error bars are based on 0.5 h air temperatures as experimental unit ($n = 48$).

3.5. Leaf Respiration

The diurnal and seasonal variations in the leaf respiration rate related well with the corresponding variation in air temperature (Table 1). The minimum leaf respiration for trees, shrubs, and herbs all appeared in March, rose sharply until July, and then decreased until November (Figure 4). Shrub leaves per unit of biomass had slightly higher respiration than tree and herb leaves. Leaf biomass increased with time (Table 3), which was consistent with the LAI measured by LAI-2000. Cumulative leaf respiration per unit of ground area for trees, shrubs, and herbs indicated that tree leaves had higher respiration than shrub and herbaceous leaves (Table 3), corresponding mainly with the highest leaf biomass for trees. Over time, the leaf respiration per unit of ground area increased.

Table 3. Leaf dry biomass ($\text{t}\cdot\text{ha}^{-1}$) and leaf respiration per ground area ($\text{g}\cdot\text{C}\cdot\text{m}^{-2}\cdot\text{y}^{-1}$) for trees, shrubs, and herbs, and leaf area index (LAI) during 2010–2013.

Items	Year				
	2010	2011	2012	2013	
Tree	Biomass	10.35 (0.86)	11.23 (0.78)	12.11 (1.14)	13.42 (1.21)
	Respiration	41.53 (3.89)	45.28 (4.15)	45.21 (3.71)	53.39 (4.82)
Shrub	Biomass	0.10 (0.04)	0.11 (0.03)	0.13 (0.02)	0.15 (0.01)
	Respiration	0.46 (0.03)	0.50 (0.04)	0.54 (0.06)	0.71 (0.08)
Herb	Biomass	0.42 (0.04)	0.45 (0.05)	0.48 (0.04)	0.51 (0.04)
	Respiration	1.28 (0.15)	1.37 (0.18)	1.40 (0.11)	1.56 (0.17)
All	Biomass	10.87 (1.04)	11.79 (0.82)	12.72 (1.14)	14.08 (1.31)
	Respiration	43.27 (3.92)	47.15 (4.27)	47.15 (4.11)	55.66 (4.52)
LAI		2.15 (0.56)	2.47 (0.62)	2.74 (0.46)	3.15 (0.48)

Note: standard error is provided in brackets.

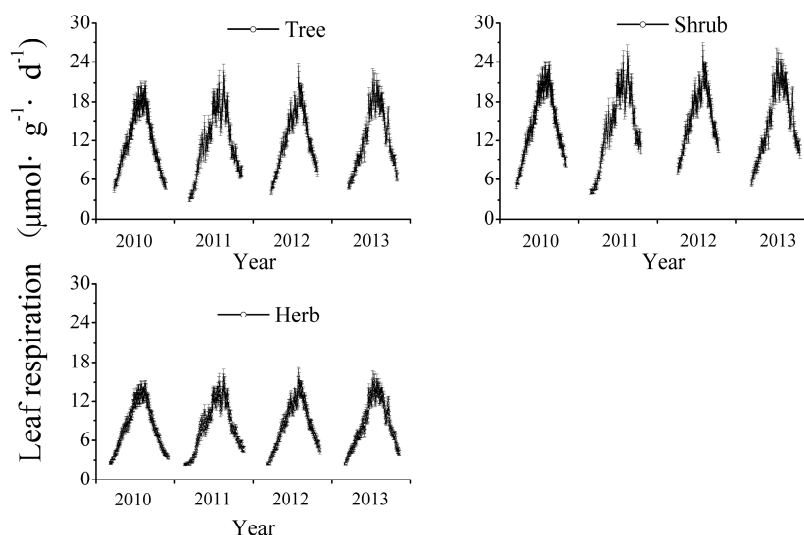


Figure 4. Daily mean leaf respiration for trees, shrubs, and herbs in the *L. principis-rupprechtii* forest during 2010–2013. Error bars are based on 0.5 h air temperatures as experimental unit ($n = 48$).

3.6. Ecosystem Respiration

The minimum ecosystem respiration appeared in January–March, rose sharply until July, and then decreased until winter (Figure 5). Ecosystem respiration ranged from 0.22 ± 0.02 to $7.86 \pm 0.38 \mu\text{mol}\cdot\text{m}^{-2}\cdot\text{s}^{-1}$ in 2010–2013. The component respiration demonstrated a similar seasonal variation with ecosystem respiration. Soil was the strongest source of annual respiration for the

ecosystem, which was approximately 50 times higher than the minimum respiration for CWD (Table 4). Soil, CWD, stem, leaf, and ecosystem respiration in 2013 was the highest among 2010–2013. Aboveground autotrophic respiration (stem + leaf respiration) comprised 10.26% of the total respiration, with leaf respiration slightly higher than stem respiration.

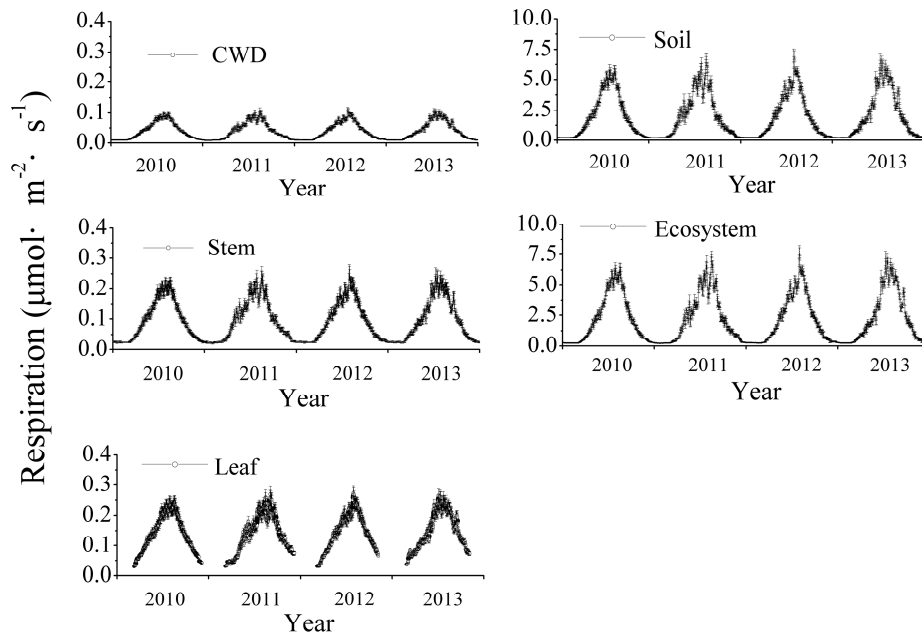


Figure 5. Daily mean soil, CWD, stem, leaf, and total ecosystem respiration in the *L. principis-rupprechtii* forest during 2010–2013. Error bars are based on 0.5 h soil temperatures and air temperatures as experimental unit, respectively ($n = 48$).

Table 4. Ecosystem respiration, component respiration ($\text{g}\cdot\text{C}\cdot\text{m}^{-2}\cdot\text{y}^{-1}$), and percentage (%) during 2010–2013 and the average over four years.

Year	Soil	CWD	Stem	Leaf	Ecosystem
2010	710.37 (20.14)	14.57 (1.58)	33.52 (2.86)	43.27 (3.92)	801.73 (58.67)
Percentage	88.60%	1.82%	4.18%	5.40%	100%
2011	721.45 (22.45)	15.30 (1.35)	34.68 (3.18)	47.15 (4.27)	818.58 (68.14)
Percentage	88.13%	1.87%	4.24%	5.76%	100%
2012	692.77 (19.64)	15.20 (1.61)	34.12 (2.17)	47.15 (4.11)	789.24 (51.55)
Percentage	87.78%	1.93%	4.32%	5.97%	100%
2013	737.27 (24.27)	16.56 (1.48)	38.82 (3.22)	55.66 (4.52)	848.31 (74.12)
Percentage	86.91%	1.95%	4.58%	6.56%	100%
Average	715.47 (28.48)	15.41 (1.72)	35.28 (4.78)	48.31 (5.24)	814.47 (64.22)
Percentage	87.85%	1.89%	4.33%	5.93%	100%

Note: standard error is provided in brackets.

3.7. Net Primary Productivity

The carbon content ratio was measured to calculate the carbon density, and the carbon content ratio was different in various components of vegetation in the *L. principis-rupprechtii* forest (Table S9). NPP was highest in 2013 ($833.33 \pm 80.14 \text{ g}\cdot\text{C}\cdot\text{m}^{-2}\cdot\text{y}^{-1}$), with an average of $817.16 \pm 81.48 \text{ g}\cdot\text{C}\cdot\text{m}^{-2}\cdot\text{y}^{-1}$ in the *L. principis-rupprechtii* forest, of which ΔB_{living} and D_{total} accounted for 77.7%, and 22.3%, respectively (Table 5). NEE was the lowest in 2012 ($-344.14 \pm 22.32 \text{ g}\cdot\text{C}\cdot\text{m}^{-2}\cdot\text{y}^{-1}$), and the average in all years was $-336.71 \pm 25.15 \text{ g}\cdot\text{C}\cdot\text{m}^{-2}\cdot\text{y}^{-1}$, which revealed a carbon sink in the *L. principis-rupprechtii* forest.

Table 5. Annual net primary productivity (NPP) and net ecosystem exchange (NEE) during 2010–2013 ($\text{g}\cdot\text{C}\cdot\text{m}^{-2}\cdot\text{y}^{-1}$).

Items	2010	2011	2012	2013	Average
ΔB_{living}	656.48 (51.22)	623.35 (52.25)	605.88 (51.14)	654.15 (53.33)	634.97 (52.52)
D_{total}	155.04 (12.85)	190.82 (18.17)	203.76 (18.82)	179.18 (15.69)	182.19 (16.85)
NPP	811.52 (72.28)	814.17 (67.58)	809.64 (72.66)	833.33 (80.14)	817.16 (81.48)
NEE	−335.21 (20.52)	−329.93 (19.64)	−344.14 (22.32)	−337.55 (17.34)	−336.71 (25.15)

Note: standard error is provided in brackets.

3.8. Comparison between Biometric and Eddy Covariance Measurements

Eddy covariance measurements of NEE showed seasonal variation, with a maximum in November ($2.71 \pm 0.22 \text{ g}\cdot\text{C}\cdot\text{m}^{-2}\cdot\text{d}^{-1}$) and a minimum in August ($-6.84 \pm 0.56 \text{ g}\cdot\text{C}\cdot\text{m}^{-2}\cdot\text{d}^{-1}$) (Figure 6). Eddy covariance measurements of NEE from May to September were negative, which suggested a carbon sink during the growing season. Overall, eddy covariance measurements of NEE showed an average of $-288.33 \pm 25.26 \text{ g}\cdot\text{C}\cdot\text{m}^{-2}\cdot\text{y}^{-1}$ ($-292.28 \pm 18.17 \text{ g}\cdot\text{C}\cdot\text{m}^{-2}\cdot\text{y}^{-1}$, $-281.02 \pm 17.22 \text{ g}\cdot\text{C}\cdot\text{m}^{-2}\cdot\text{y}^{-1}$, $-270.56 \pm 20.21 \text{ g}\cdot\text{C}\cdot\text{m}^{-2}\cdot\text{y}^{-1}$, and $-309.47 \pm 24.37 \text{ g}\cdot\text{C}\cdot\text{m}^{-2}\cdot\text{y}^{-1}$ for 2010 to 2013, respectively), which indicated a sink at this site. These numbers are close to the results from the biometric measurements but average 14% higher. Based on eddy covariance measurements, annual ecosystem respiration was estimated as $780.37 \pm 82.18 \text{ g}\cdot\text{C}\cdot\text{m}^{-2}\cdot\text{y}^{-1}$ ($759.12 \pm 62.51 \text{ g}\cdot\text{C}\cdot\text{m}^{-2}\cdot\text{y}^{-1}$, $766.38 \pm 71.17 \text{ g}\cdot\text{C}\cdot\text{m}^{-2}\cdot\text{y}^{-1}$, $781.49 \pm 64.82 \text{ g}\cdot\text{C}\cdot\text{m}^{-2}\cdot\text{y}^{-1}$, and $814.48 \pm 75.18 \text{ g}\cdot\text{C}\cdot\text{m}^{-2}\cdot\text{y}^{-1}$ for 2010 to 2013, respectively). Daily mean ecosystem respiration based on chamber measurements and eddy covariance measurements are plotted in Figure 7. The curve shows a good correlation between these two measurement methods, with $R^2 = 0.93$.

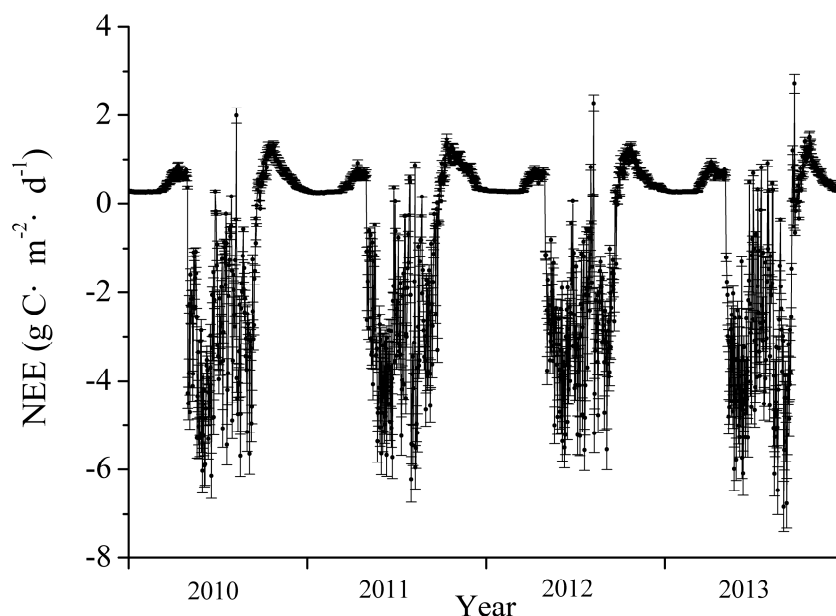


Figure 6. Eddy covariance measurements of NEE in the *L. principis-rupprechtii* forest. Data are daily mean NEE during 2010–2013. Error bars are based on 0.5 h eddy covariance measurements of NEE as experimental unit ($n = 48$).

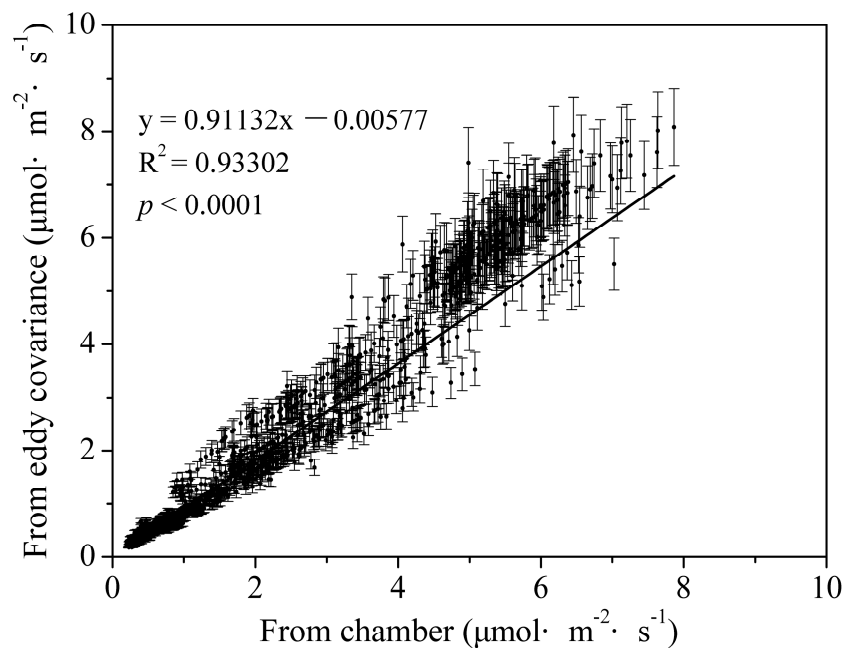


Figure 7. Comparison between chamber-based and eddy covariance measurements of ecosystem respiration. Data are daily mean respiration during 2010–2013. The solid line indicates a linear fit.

4. Discussion

The seasonal variation of component respiration was driven by temperature, and temperature was strongly exponentially correlated with component respiration. This conclusion has been reported in several studies [16,26]. According to our analysis, the ecosystem respiration based on eddy covariance measurements was also exponentially related to the air temperature, explaining 94% of the variability in the ecosystem respiration (Figure S10).

Biometric-based flux measurements combined with spatial and temporal upscaling allowed us to estimate the respiration of each component of the ecosystem. The CO_2 flux of soil from our site was higher than that from a mature temperate mixed forest in the Changbai Mountains ($0.49\text{--}4.12 \mu\text{mol}\cdot\text{m}^{-2}\cdot\text{s}^{-1}$), which may be due to the higher temperature at our site (Annual average temperature is 3.6°C in the Changbai Mountains) [26]. Soil respiration is influenced by many factors, including abiotic factors, such as the soil temperature, soil moisture, rainfall, and soil C/N, and biotic factors, such as vegetation cover, litter thickness on the ground, fine root mass, soil organic matter, soil characteristics, leaf area index, and human activities. A number of studies concluded that soil moisture is an important factor influencing soil respiration [42–44]. However, a comparison of recent findings in this region showed that soil moisture had little impact on soil respiration relative to in situ temperature. An adequate soil moisture level may explain the non-significant influence of soil moisture on soil respiration [26]. The Q_{10} value was the highest in soil respiration, with a value of 4.19, which revealed that there was a stronger sensitivity of soil respiration to temperature in different component respirations, which was different from other ecosystems. For example, Raich and Schlesinger reviewed global soil respiration values and found a median Q_{10} value of 2.4 [45]. In a temperate mixed-hardwood forest, the Q_{10} value ranged from 3.4 to 5.6 [46]. The Q_{10} value ranged from 1.93 to 4.80 in different vegetation communities in the Belgian Campine region [47]. Moreover, Cao et al. reported Q_{10} values of 2.75 and 3.22 in an alpine meadow on the Tibetan Plateau of China [48]. Wu et al. reported a value of 4.07 in the Changbai Mountains of China [49]. On the eastern part of the Loess Plateau of China, the Q_{10} value ranged from 2.37 to 5.53 [50]. The various Q_{10} values reported in different ecosystems may be due to both methodology and differences in biotic and abiotic factors that affect soil respiration differently [50].

Whole-ecosystem respiration is dominated by soil respiration in forests [4]. Soil respiration has been found to account for 30–90% of total ecosystem respiration in temperate forests [13], and our result was close to the upper limit, at 87.85%. The percentage of soil respiration was higher, possibly due to the lower precipitation (600 mm) at our site, but there were lower nutrients in the soil (sandy loam) at a Michigan site and in a ponderosa pine forest in Oregon (76%) [37]. Total soil respiration is always regarded as a critical component of the carbon balance of an ecosystem. The estimated annual soil respiration was $715.47 \pm 28.48 \text{ g}\cdot\text{C}\cdot\text{m}^{-2}\cdot\text{y}^{-1}$, which was similar to that reported by Raich and Schlesinger for temperate coniferous forests, at $681 \pm 95 \text{ g}\cdot\text{C}\cdot\text{m}^{-2}\cdot\text{y}^{-1}$ [45]. Other ecosystems reported various values for soil respiration, including 600–700 $\text{g}\cdot\text{C}\cdot\text{m}^{-2}\cdot\text{y}^{-1}$ in beech forests in France [51], 485 $\text{g}\cdot\text{C}\cdot\text{m}^{-2}\cdot\text{y}^{-1}$ in hardwood forests in the USA [52], 581 $\text{g}\cdot\text{C}\cdot\text{m}^{-2}\cdot\text{y}^{-1}$ in a warm-temperate mixed forest in Japan [53], 963.98 $\text{g}\cdot\text{C}\cdot\text{m}^{-2}\cdot\text{y}^{-1}$ in a Korean pine and broadleaf mixed forest in China [54], and 454 $\text{g}\cdot\text{C}\cdot\text{m}^{-2}\cdot\text{y}^{-1}$ in a tropical seasonal rainforest in China [55]. These different results demonstrate that soil respiration is closely related to vegetation and climate.

In our study, leaf respiration was second in magnitude among the respiration fractions. This result is consistent with that of previous studies [5,26]. However, the leaf respiration at our site was lower than that in an old-growth hardwood forest ($114.85 \text{ g}\cdot\text{C}\cdot\text{m}^{-2}\cdot\text{y}^{-1}$) and a hemlock forest ($72.20 \text{ g}\cdot\text{C}\cdot\text{m}^{-2}\cdot\text{y}^{-1}$) in the USA [16]. Moreover, Law et al. compared leaf respiration in young ($124 \text{ g}\cdot\text{C}\cdot\text{m}^{-2}\cdot\text{y}^{-1}$) and old ($136 \text{ g}\cdot\text{C}\cdot\text{m}^{-2}\cdot\text{y}^{-1}$) ponderosa pine forests of the USA [56], which were all higher than ours. In the present study, this lower leaf respiration may have been caused by (1) the lower annual mean LAI (4.1 in the hardwood forest and 3.8 in the hemlock forest), (2) reduced air temperature and photosynthetic active radiation [57], or (3) decreased foliage N and chlorophyll concentrations [37]. In addition, both the canopy position and foliage age had significant effects on leaf respiration [12].

Because of difficulties in measurement, little attention was paid to stem respiration in the past. However, with increasing atmospheric CO_2 concentrations and as an important part of the annual carbon balance of forest ecosystems, studies of stem respiration have generated active debate. Stem respiration was strongly correlated with temperature, and the Q_{10} value at our site was similar to that of other ecosystems. For example, in a *Pinus koraiensis* forest in China, the Q_{10} value ranged from 2.56 to 3.32 [58]. In a temperate mixed forest in China, the Q_{10} value ranged from 1.86 to 2.41 [26]. Ryan et al. reported that the Q_{10} value ranged from 1.3 to 1.9 in four conifer forests in the USA [59]. According to our study, stem respiration was slightly lower than leaf respiration, which was consistent with others [5,26,37,38]. However, the stem respiration at our site was much lower than those in an old-growth hardwood forest ($130.5 \text{ g}\cdot\text{C}\cdot\text{m}^{-2}\cdot\text{y}^{-1}$) and a hemlock forest ($206.5 \text{ g}\cdot\text{C}\cdot\text{m}^{-2}\cdot\text{y}^{-1}$) in the USA [16], which may be due to lower sapwood volume ($296.3 \text{ m}^3\cdot\text{ha}^{-1}$ in the hardwood forest and $448.5 \text{ m}^3\cdot\text{ha}^{-1}$ in the hemlock forest). In addition, stem respiration is influenced by numerous factors, including meteorological factors (e.g., stem temperature, CO_2 concentration, and humidity) and biological factors (tree species, tree age, diameter at breast height, sapwood size, and nitrogen content in the stem). Latitude, altitude, and topographic factors indirectly influence respiration rates through meteorological or biological factors [60]. Moreover, scaling up based on measurements of the stem respiration rate and sapwood volume may underestimate total stem respiration rates because younger woody tissues have higher respiration rates [38]. Future studies are required to develop a more accurate scaling-up scheme.

In general, CWD has high ecological relevance, contributes significantly to crucial ecological processes in forest ecosystems, and plays an essential role in carbon pools [61]. Furthermore, CWD respiration as a component of ecosystem respiration is essential to determining a forest's carbon budget [62]. However, few studies of CWD respiration have been conducted in most forest types [63]. In particular, quantification of the contribution of CWD respiration to total ecosystem respiration in the Qinling Mountains has not been previously conducted. Our study showed that the seasonality of CWD respiration was mainly driven by the CWD temperature and showed an overall bell-shaped curve for all five decay classes. This conclusion is corroborated by previous studies [64,65]. The Q_{10} ranged from 1.7 to 4.1 for different decay classes in various ecosystems [62,65], and our result fell within this range.

Moreover, Wu et al. reported that the Q_{10} value ranged from 2.41 to 2.95 in the Changbai Mountains of China [66]. In a montane moist evergreen broadleaf forest of China, the Q_{10} value ranged from 1.73 to 2.08 [67]. Furthermore, the Q_{10} value was significantly affected by the temperature ranges. For example, the Q_{10} value was 4.1 for 5–20 °C and 1.7 for 20–42 °C in a boreal black spruce forest in Canada [65].

CWD respiration is a complex process that depends on many factors, including tree species, temperature, moisture, substrate quality, diameter class, and decomposer type [68,69]. According to our study, the annual CWD respiration was much lower than that in an old-growth Amazonian forest ($171.8 \text{ g}\cdot\text{C}\cdot\text{m}^{-2}\cdot\text{y}^{-1}$) [70], which may be mainly caused by the reduced CWD biomass at our site. Meanwhile, the annual CWD respiration was slightly lower than that in an old-growth hardwood forest ($43 \text{ g}\cdot\text{C}\cdot\text{m}^{-2}\cdot\text{y}^{-1}$) and a hemlock forest ($29 \text{ g}\cdot\text{C}\cdot\text{m}^{-2}\cdot\text{y}^{-1}$) in the USA [16]. The reason for higher annual CWD respiration in hardwood and hemlock forests may be the surface area of CWD for upscaling [16]. In our study, we quantified the CWD into five decay classes. The CWD respiration rates measured per unit volume might underestimate the CWD respiration rates, whereas CWD respiration rates measured per unit surface area might overestimate the CWD respiration rates. A large log may have large volume but smaller surface area than many small logs. As such, the conversion of CWD respiration rates measured per unit area to rates per unit volume might be more appropriate to CWD respiration in this forest. Moreover, to upscale chamber measurements of CWD respiration to the stand level, the volume was more convenient and accurate than the surface area. Measuring the CWD respiration accurately is important for estimating forest ecosystem respiration. Thus, further research should be done by using the surface area or volume of CWD for upscaling. In addition, future studies are necessary to measure CWD respiration in different diameter classes.

Daily mean ecosystem respiration measured from eddy covariance and chamber methods was shown in Figure 7. The eddy covariance (y) and chamber (x) methods were in better agreement after adjusting the CO_2 flux in this forest using the equation $y = 0.91132x - 0.00577$ (Figure 7). The comparisons between chamber and eddy covariance ecosystem respiration measurements were more consistent than in other studies [71,72]. Our result showed that the daily mean ecosystem respiration upscaled from chamber measurements agreed well with eddy covariance measurements, with $R^2 = 0.93$, which was similar to that of an old-growth forest in the Great Lakes region of the USA [16], with $R^2 = 0.96$, although some studies suggested that the result from chamber measurements was higher than that from eddy covariance measurements [37,73].

An annual average ecosystem respiration of $780.37 \pm 82.18 \text{ g}\cdot\text{C}\cdot\text{m}^{-2}\cdot\text{y}^{-1}$ was calculated from eddy covariance measurements. Based on chamber measurements, the corresponding value was $814.47 \pm 64.22 \text{ g}\cdot\text{C}\cdot\text{m}^{-2}\cdot\text{y}^{-1}$. Our result is very close to that in a boreal black spruce forest in Canada, which had a range of 790–890 $\text{g}\cdot\text{C}\cdot\text{m}^{-2}\cdot\text{y}^{-1}$ [74]. However, ecosystem respiration from our site was much lower than that from old-growth Amazon tropical forests, with an estimate of $2337.6 \text{ g}\cdot\text{C}\cdot\text{m}^{-2}\cdot\text{y}^{-1}$ [75]. Higher temperatures, longer growing seasons, and higher photosynthesis and growth rates in tropical forests may explain the higher respiration than that from our temperate coniferous forests.

Our study found that the annual average ecosystem respiration measured by the chamber method was 5% higher than that measured by the eddy covariance. The error sources for explaining this discrepancy are complicated. Firstly, chambers may disturb the environment and alter CO_2 concentrations, as well as pressure gradients, turbulent fluctuations, and air flow. Thus, they may interfere with the production and transport of CO_2 [26]. Closed chambers completely cover the ecosystem during the measurement process and thereby alter the natural long-wave radiation balance to almost zero. This causes reduced surface cooling, weak development of stable stratification, and, finally, higher respiration than those obtained via eddy covariance measurements [76]. Secondly, our annual average ecosystem respiration estimates based on chamber measurements may have uncertainties. One possible source of uncertainty is in the method of extrapolating a temperature-respiration relationship to the winter. Under a 95% confidence interval, the uncertainties

in predicting daily mean soil respiration, CWD respiration, stem respiration, and leaf respiration averaged 10%, 8%, 12%, and 14%, respectively, of the predicted values. The uncertainties may also derive from the estimation of CWD and stem volumes, the dry leaf biomass, and the chamber upscaling processes. Thirdly, nocturnal eddy covariance measurements with low friction velocity, extrapolation of nighttime respiration to daytime respiration may underestimate the ecosystem respiration by the eddy covariance method. Annual NEE estimates were as high as $-336.71 \pm 25.15 \text{ g}\cdot\text{C}\cdot\text{m}^{-2}\cdot\text{y}^{-1}$ from biometric measurements but $-288.33 \pm 25.26 \text{ g}\cdot\text{C}\cdot\text{m}^{-2}\cdot\text{y}^{-1}$ from eddy covariance measurements. Our results revealed that this site was a carbon sink, which was consistent with the findings of Zhou et al. [11]; they found that a carbon sink in a *L. principis-rupprechtii* forest in China was $-271 \text{ g}\cdot\text{C}\cdot\text{m}^{-2}\cdot\text{y}^{-1}$. Meanwhile, our estimations of NEE fall well within the range reported between -70 and $-740 \text{ g}\cdot\text{C}\cdot\text{m}^{-2}\cdot\text{y}^{-1}$ for temperate forests [15,77].

Our study found that the NEE measured by the eddy covariance method was 14% higher than that measured by the biometric, which is consistent with Wang et al. [26]. However, our study showed that the discrepancy was lower than that of Wang et al. (22.5%), and the mean difference ($48.38 \pm 9.67 \text{ g}\cdot\text{C}\cdot\text{m}^{-2}\cdot\text{y}^{-1}$) was also lower than that of temperate forests ($100 \text{ g}\cdot\text{C}\cdot\text{m}^{-2}\cdot\text{y}^{-1}$) [78], which indicated that these two methods had good agreement in measuring the NEE in this forest. However, there was still a discrepancy between the biometric and eddy covariance measurements, which may be due to the complicated error sources.

The error in the result from both biometric and eddy covariance was associated with sampling methods of flux measurement [30]. Ehman et al. concluded that the largest error source in the biometric method may be attributable to sampling (that is, inter-plot variability) [79]. All natural ecosystems are heterogeneous at some scale, and so the question arises whether estimation of fluxes based on a limited number of samples represents the average of the total ecosystem. In our study, the sampling error included estimating the NPP for sampling the trees, shrubs, herbs, fine roots, and litterfall. Additionally, we used soil collars to measure R_S and R_R and sampled the CWD to measure R_{CWD} , which all may produce the sampling error. In addition, Ohtsuka et al. considered that the topography may introduce sampling errors when estimating the NEE based on the eddy covariance method [30].

Another error was more likely to be related to estimation of NPP. Although Ohtsuka et al. deemed annual forest census within a large permanent plot and adequate number of litter traps for detritus production to be the most suitable method for measuring NPP [30], there were still some uncertainties. One possible uncertainty was derived from the biomass regression model. Under a 95% confidence interval, the uncertainties in predicting tree and shrub biomass averaged 8% and 14%, respectively, of the predicted values. Clark et al. considered that using off-site allometric equations could alter NPP by as much as 20% [80]. Also, these allometric relationships do not take into account seasonal changes in wood C concentration that may occur. Our study showed that the carbon content ratio values were diverse among varying plant species and different organs in the same plant (Table S9). However, many researchers used 50% as the carbon content ratio [81,82], which would overestimate the NPP by 7.4% in this forest. D_{total} is an important component of NPP; a study by Curtis et al. revealed that the detritus made up nearly two-thirds of the annual C production [77]. However, in our study, we found the D_{total} accounted for less than a quarter of NPP. CWD as a part of D_{total} can be difficult to measure precisely due to the heterogeneous distribution of forest floor detritus [79,80,83], which was the largest source of uncertainty in the estimation of NPP. However, we have adequately quantified annual variability in CWD production according to the annual forest census. Moreover, underestimation could have been caused by minor NPP components typically neglected (for example, root exudation, net accumulation of non-structural carbohydrates, herbivory consumption, production of volatile organic compounds [78,80]), which in general contribute between 1% and 4% of NPP [84]. In addition, Ohtsuka et al. considered that the estimation of R_{CWD} represented a critical source of potential error [30]; few studies have measured the R_{CWD} . Ehman et al. reported the R_{CWD} was 7% of R_S [79], but this proportion was only 2% in our study. We quantified the CWD into five decay classes to obtain more accurate measurements of R_{CWD} . However, the respirations of CWD at different diameter

classes and fine woody debris (1 cm \leq diameter < 10 cm) were not measured, which may result in a lower observed R_{CWD} at this site.

The permanent plot was protected by an enclosure, and this site was level (a mean slope of 5°), and the overstory and understory of the forest were homogeneous, which are ideal conditions for measuring the NEE using the eddy covariance method in this forest. However, there were still error sources for measuring the NEE based on eddy covariance measurements. In our study, these eddy covariance error sources mainly include a double-directional interpolation model of artificial neural networks (ANNs) to fill the gaps, nocturnal low friction velocity, and the extrapolation of nighttime respiration from the eddy covariance measurements to daytime respiration.

5. Conclusions

This paper presents the first set of results (2010–2013) from a long-term project measuring forest-atmosphere CO₂ exchanges using eddy covariance and biometric methods simultaneously in a *L. principis-rupprechtii* forest. In our study, temperature was the primary controlling factor for respiration in this forest. Exponential functions explained most of the observed temporal variations in respiration in response to temperature. Based on the chamber upscale processes, we obtained the cumulative annual ecosystem respiration ($814.47 \pm 64.22 \text{ g}\cdot\text{C}\cdot\text{m}^{-2}\cdot\text{y}^{-1}$), but this number was 5% higher than that from the eddy covariance measurements. We considered this small discrepancy to have arisen mainly because the respiration of CWD at different diameter classes and fine woody debris (1 cm \leq diameter < 10 cm) was not measured due to the possible uncertainty in the method of extrapolating a temperature-respiration relationship to the winter and due to the uncertainties in the estimation of CWD and stem volumes, dry leaf biomass, and the chamber upscale processes.

Using measurements of the NPP ($817.17 \pm 81.48 \text{ g}\cdot\text{C}\cdot\text{m}^{-2}\cdot\text{y}^{-1}$) combined with the heterotrophic respiration based on the chamber method ($480.45 \pm 52.24 \text{ g}\cdot\text{C}\cdot\text{m}^{-2}\cdot\text{y}^{-1}$), we obtained the NEE ($-336.71 \pm 25.15 \text{ g}\cdot\text{C}\cdot\text{m}^{-2}\cdot\text{y}^{-1}$) in this forest. This result was close to that from eddy covariance measurements ($-288.33 \pm 25.26 \text{ g}\cdot\text{C}\cdot\text{m}^{-2}\cdot\text{y}^{-1}$), which indicated that these two methods had good agreement in measuring the NEE in this forest. In our study, we calibrated the instruments periodically, repeatedly measured a variety of respiration components for 4 years, reduced the disturbance of chamber measurements, quantified the CWD into five decay classes, and measured the carbon content ratio of various components, all of which can enhance the consistency of the eddy covariance and the biometric fluxes. However, there was still a 14% discrepancy between the biometric and eddy covariance measurements, which may be due to the complicated error sources. Thus, more detailed experiments and related theoretical studies are needed in the future.

Supplementary Materials: The following are available online at <http://www.mdpi.com/1999-4907/9/2/67/s1>, Figure S1: Some photos of *L. principis-rupprechtii* forest and flux tower in this region, Table S1: The regression model of biomass, volume, and height of *L. principis-rupprechtii*, Table S2: The regression model of shrub biomass in the *L. principis-rupprechtii* forest, Table S3: CWD characteristics of different decay classes in forest system, Figure S2: The relationship between temperature of different CWD decay classes and 10 cm soil temperature, Figure S3: The relationship between air temperature and stem temperature, Figure S4: Daily mean air temperature and 10 cm soil temperature in the *L. principis-rupprechtii* forest during 2010–2013, Figure S5: Daily mean photosynthetically active radiation in the *L. principis-rupprechtii* forest during 2010–2013, Table S4: Average carbon content ratio of litterfall and various organs of trees, shrubs, and herbs in the *L. principis-rupprechtii* forest (%), Figure S6: The relationship between ecosystem respiration based on eddy covariance measurement and air temperature. Data shown are daily means during 2010–2013.

Acknowledgments: We are grateful to the Qinling National Forest Ecosystem Research Station for providing some data and the experimental equipment. This research was funded by the project “Technical management system for increasing the capacity of carbon sink and water regulation of mountain forests in the Qinling Mountains” (201004036) of the State Forestry Administration of China.

Author Contributions: J.Y. and S.Z. conceived and designed the experiments; J.Y., Z.H., and J.P. performed the experiments; J.Y. analyzed the data; L.H. contributed reagents/materials/analysis tools; J.Y. and S.J. wrote the paper.

Conflicts of Interest: The authors declare no conflict of interest.

References

1. Post, W.M.; Peng, T.H.; Emanuel, W.R.; King, A.W.; Dale, V.H.; Angelis, D.L. The global carbon cycle. *Am. Sci.* **1990**, *78*, 310–326.
2. Conway, T.J.; Tans, P.P.; Waterman, L.S.; Thoning, K.W.; Kitzis, D.R.; Masarie, K.A.; Ni, Z. Evidence for interannual variability of the carbon cycle from the National Oceanic and Atmospheric Administration/Climate Monitoring and Diagnostics Laboratory Global Air Sampling Network. *J. Geophys. Res.* **1994**, *99*, 22831–22855. [[CrossRef](#)]
3. Houghton, R.; Hackler, J.; Lawrence, K. The US carbon budget: Contributions from land-use change. *Science* **1999**, *285*, 574–578. [[CrossRef](#)] [[PubMed](#)]
4. Bolstad, P.; Davis, K.; Martin, J.; Cook, B.; Wang, W. Component and whole-system respiration fluxes in northern deciduous forests. *Tree Physiol.* **2004**, *24*, 493–504. [[CrossRef](#)] [[PubMed](#)]
5. Guan, D.X.; Wu, J.B.; Zhao, X.S.; Han, S.J.; Yu, G.R.; Sun, X.M.; Jin, C.J. CO₂ fluxes over an old, temperate mixed forest in northeastern China. *Agric. For. Meteorol.* **2006**, *137*, 138–149. [[CrossRef](#)]
6. Kang, Y.X.; Chen, Y.P. Woody plant flora of Huoditang forest region. *J. Northwest For. Coll.* **1996**, *11*, 1–10. (In Chinese)
7. Schröter, D.; Cramer, W.; Leemans, R.; Prentice, I.C.; Araújo, M.B.; Arnell, N.W.; Bondeau, A.; Bugmann, H.; Carter, T.R.; Gracia, C.A.; et al. Ecosystem service supply and vulnerability to global change in Europe. *Science* **2005**, *310*, 1333–1337. [[CrossRef](#)] [[PubMed](#)]
8. Etzold, S.; Ruehr, N.K.; Zweifel, R.; Dobbertin, M.; Zingg, A.; Pluess, P.; Häsler, R.; Eugster, W.; Buchmann, N. The carbon balance of two contrasting mountain forest ecosystems in Switzerland: Similar annual trends, but seasonal differences. *Ecosystems* **2011**, *14*, 1289–1309. [[CrossRef](#)]
9. Leng, W.; He, H.S.; Bu, R.; Dai, L.; Hu, Y.; Wang, X. Predicting the distributions of suitable habitat for three larch species under climate warming in Northeastern China. *For. Ecol. Manag.* **2008**, *254*, 420–428. [[CrossRef](#)]
10. Lei, R.D.; Dang, K.L.; Zhang, S.X.; Tan, F.L. Effect of a *Larix principis-rupprechtii* forest plantation on soil in middle zone of south-facing slope of the Qinling mountains. *Sci. Silvae Sin.* **1997**, *33*, 463–470. (In Chinese)
11. Zhou, Y.R.; Yu, Z.L.; Zhao, S.D. Carbon storage and budget of major Chinese forest types. *Chin. J. Plant Ecol.* **2000**, *24*, 518–522. (In Chinese)
12. Brooks, J.R.; Hinckley, T.M.; Ford, E.D.; Sprugel, D.G. Foliage dark respiration in *Abies amabilis* (Dougl.) Forbes: Variation within the canopy. *Tree Physiol.* **1991**, *9*, 325–338. [[CrossRef](#)] [[PubMed](#)]
13. Valentini, R.; Matteucci, G.; Dolman, A.J.; Schulze, E.D.; Rebmann, C.; Moors, E.J.; Granier, A.; Gross, P.; Jensen, N.O.; Pilegaard, K.; et al. Respiration as the main determinant of carbon balance in European forests. *Nature* **2000**, *404*, 861–865. [[CrossRef](#)] [[PubMed](#)]
14. Malhi, Y.; Baldocchi, D.D.; Jarvis, P.G. The carbon balance of tropical, temperate and boreal forests. *Plant Cell Environ.* **1999**, *22*, 715–740. [[CrossRef](#)]
15. Baldocchi, D.D.; Wilson, K.B. Modeling CO₂ and water vapor exchange of a temperate broadleaved forest across hourly to decadal time scales. *Ecol. Model.* **2001**, *142*, 155–184. [[CrossRef](#)]
16. Tang, J.; Bolstad, P.V.; Desai, A.R.; Martin, J.G.; Cook, B.D.; Davis, K.J.; Carey, E.V. Ecosystem respiration and its components in an old-growth forest in the Great Lakes region of the United States. *Agric. For. Meteorol.* **2008**, *148*, 171–185. [[CrossRef](#)]
17. Khomik, M.; Arain, M.A.; Brodeur, J.J.; Peichl, M.; Restrepo Coupé, N.; McLaren, J.D. Relative contributions of soil, foliar, and woody tissue respiration to total ecosystem respiration in four pine forests of different ages. *J. Geophys. Res. Biogeosci.* **2015**, *115*, 4209–4224. [[CrossRef](#)]
18. Grace, J.; Lloyd, J.; McIntyre, J.; Miranda, A.C.; Meir, P.; Miranda, H.S.; Nobre, C.; Moncrieff, J.; Massheder, J.; Malhi, Y. Carbon dioxide uptake by an undisturbed tropical rain forest in southwest Amazonia, 1992 to 1993. *Science* **1995**, *270*, 778–780. [[CrossRef](#)]
19. Black, T.A.; Den Hartog, G.; Neumann, H.H.; Blanken, P.D.; Yang, P.C.; Russell, C.; Nesic, Z.; Lee, X.; Chen, S.G.; Staebler, R.; et al. Annual cycles of water vapour and carbon dioxide fluxes in and above a boreal aspen forest. *Glob. Chang. Biol.* **1996**, *2*, 219–229. [[CrossRef](#)]
20. Luyssaert, S.; Reichstein, M.; Schulze, E.D.; Janssens, I.A.; Law, B.E.; Papale, D.; Dragoni, D.; Goulden, M.L.; Granier, A.; Kutsch, W.L. Toward a consistency cross-check of eddy covariance flux-based and biometric estimates of ecosystem carbon balance. *Glob. Biogeochem. Cycles* **2009**, *23*, 1159–1171. [[CrossRef](#)]

21. Speckman, H.N.; Frank, J.M.; Bradford, J.B.; Miles, B.L.; Massman, W.J.; Parton, W.J.; Ryan, M.G. Forest ecosystem respiration estimated from eddy covariance and chamber measurements under high turbulence and substantial tree mortality from bark beetles. *Glob. Chang. Biol.* **2015**, *21*, 708–721. [[CrossRef](#)] [[PubMed](#)]
22. Goulden, M.L.; Munger, J.W.; Fan, S.M.; Daube, B.C.; Wofsy, S.C. Exchange of carbon dioxide by a deciduous forest: Response to interannual climate variability. *Science* **1996**, *271*, 1576–1578. [[CrossRef](#)]
23. Billesbach, D. Estimating uncertainties in individual eddy covariance flux measurements: A comparison of methods and a proposed new method. *Agric. For. Meteorol.* **2011**, *151*, 394–405. [[CrossRef](#)]
24. Davidson, E.; Savage, K.; Verchot, L.; Navarro, R. Minimizing artifacts and biases in chamber-based measurements of soil respiration. *Agric. For. Meteorol.* **2002**, *113*, 21–37. [[CrossRef](#)]
25. Myklebust, M.C.; Hippias, L.E.; Ryel, R.J. Comparison of eddy covariance, chamber, and gradient methods of measuring soil CO₂ efflux in an annual semi-arid grass, *Bromus tectorum*. *Agric. For. Meteorol.* **2008**, *148*, 1894–1907. [[CrossRef](#)]
26. Wang, M.; Guan, D.X.; Han, S.J.; Wu, J.L. Comparison of eddy covariance and chamber-based methods for measuring CO₂ flux in a temperate mixed forest. *Tree Physiol.* **2010**, *30*, 149–163. [[CrossRef](#)] [[PubMed](#)]
27. Dou, Z.Y.; Liu, J.J. Application of artificial neural networks to interpolation and extrapolation of flux data. *J. Northwest For. Univ.* **2009**, *24*, 58–62. (In Chinese)
28. Chen, C.G.; Peng, H. Standing crops and productivity of the major forest-types at the Huoditang forest region of the Qinling Mountains. *J. Northwest For. Coll.* **1996**, *11*, 92–102. (In Chinese, with English Abstract)
29. Rieger, I.; Lang, F.; Kleinschmit, B.; Kowarik, I.; Cierjacks, A. Fine root and aboveground carbon stocks in riparian forests: The roles of diking and environmental gradients. *Plant Soil* **2013**, *370*, 497–509. [[CrossRef](#)]
30. Ohtsuka, T.; Mo, W.; Satomura, T.; Inatomi, M.; Koizumi, H. Biometric based carbon flux measurements and net ecosystem production (NEP) in a temperate deciduous broad-leaved forest beneath a flux tower. *Ecosystems* **2007**, *10*, 324–334. [[CrossRef](#)]
31. Stenberg, P.; Linder, S.; Smolander, H.; Flower-Ellis, J. Performance of the LAI-2000 plant canopy analyzer in estimating leaf area index of some Scots pine stands. *Tree Physiol.* **1994**, *14*, 981–995. [[CrossRef](#)] [[PubMed](#)]
32. Cutini, A.; Matteucci, G.; Mugnozza, G.S. Estimation of leaf area index with the Li-Cor LAI 2000 in deciduous forests. *For. Ecol. Manag.* **1998**, *105*, 55–65. [[CrossRef](#)]
33. Munir, T.; Khadka, B.; Xu, B.; Strack, M. Partitioning forest-floor respiration into source based emissions in a boreal forested bog: Responses to experimental drought. *Forests* **2017**, *8*. [[CrossRef](#)]
34. Ringvall, A.; Ståhl, G. Field aspects of line intersect sampling for assessing coarse woody debris. *For. Ecol. Manag.* **1999**, *119*, 163–170. [[CrossRef](#)]
35. Yan, E.R.; Wang, X.H.; Huang, J.J.; Zeng, F.R.; Gong, L. Long-lasting legacy of forest succession and forest management, characteristics of coarse woody debris in an evergreen broad-leaved forest of eastern China. *For. Ecol. Manag.* **2007**, *252*, 98–107. [[CrossRef](#)]
36. Wenger, K.F. *Forestry Handbook*; John Wiley & Sons: New York, NY, USA, 1984.
37. Law, B.E.; Ryan, M.G.; Anthoni, P.M. Seasonal and annual respiration of a ponderosa pine ecosystem. *Glob. Chang. Biol.* **1999**, *5*, 169–182. [[CrossRef](#)]
38. Xu, M.; Debiase, T.A.; Qi, Y.; Goldstein, A.; Liu, Z. Ecosystem respiration in a young ponderosa pine plantation in the Sierra Nevada Mountains, California. *Tree Physiol.* **2001**, *21*, 309–318. [[CrossRef](#)] [[PubMed](#)]
39. Webb, E.K.; Pearman, G.L.; Leuning, R. Correction of flux measurements for density effects due to heat and water vapour transfer. *Q. J. R. Meteorol. Soc.* **1980**, *106*, 85–100. [[CrossRef](#)]
40. Cook, B.D.; Davis, K.J.; Wang, W.G.; Desai, A.; Berger, B.W.; Teclaw, R.M.; Martin, J.G.; Bolstad, P.V.; Bakwin, P.S.; Yi, C.X.; et al. Carbon exchange and venting anomalies in an upland deciduous forest in northern Wisconsin, USA. *Agric. For. Meteorol.* **2004**, *126*, 271–295. [[CrossRef](#)]
41. Desai, A.R.; Bolstad, P.V.; Cook, B.D.; Davis, K.J.; Carey, E.V. Comparing net ecosystem exchange of carbon dioxide between an old-growth and mature forest in the upper Midwest, USA. *Agric. For. Meteorol.* **2005**, *128*, 33–55. [[CrossRef](#)]
42. Rey, A.; Pegoraro, E.; Tedeschi, V.; De Parri, L.; Jarvis, P.G.; Valentini, R. Annual variation in soil respiration and its components in a coppice oak forest in central Italy. *Glob. Chang. Biol.* **2002**, *8*, 851–866. [[CrossRef](#)]
43. Curiel, Y.J.; Janssens, I.A.; Carrara, A.; Meiresonne, L.; Ceulemans, R. Interactive effects of temperature and precipitation on soil respiration in a temperate maritime pine forest. *Tree Physiol.* **2003**, *23*, 1263–1270.

44. Flanagan, L.B.; Johnson, B.G. Interacting effects of temperature, soil moisture and plant biomass production on ecosystem respiration in a northern temperate grassland. *Agric. For. Meteorol.* **2005**, *130*, 237–253. [[CrossRef](#)]
45. Raich, J.W.; Schlesinger, W.H. The global carbon dioxide flux in soil respiration and its relationship to vegetation and climate. *Tellus B* **1992**, *44*, 81–99. [[CrossRef](#)]
46. Davidson, E.A.; Belt, E.; Boone, R.D. Soil water content and temperature as independent or confounded factors controlling soil respiration in a temperate mixed hardwood forest. *Glob. Chang. Biol.* **1998**, *4*, 217–227. [[CrossRef](#)]
47. Curiel, Y.J.; Janssens, I.A.; Carrara, A.; Ceulemans, R. Annual Q_{10} of soil respiration reflects plant phenological patterns as well as temperature sensitivity. *Glob. Chang. Biol.* **2004**, *10*, 161–169. [[CrossRef](#)]
48. Cao, G.M.; Tang, Y.H.; Mo, W.H.; Wang, Y.S.; Li, Y.N.; Zhao, X.Q. Grazing intensity alters soil respiration in an alpine meadow on the Tibetan plateau. *Soil Biol. Biochem.* **2004**, *36*, 237–243. [[CrossRef](#)]
49. Wu, J.B.; Guan, D.X.; Wang, M.; Pei, T.F.; Han, S.J.; Jin, C.J. Year-round soil and ecosystem respiration in a temperate broad-leaved Korean Pine forest. *For. Ecol. Manag.* **2006**, *223*, 35–44. [[CrossRef](#)]
50. Li, H.J.; Yan, J.X.; Yue, X.F.; Wang, M.B. Significance of soil temperature and moisture for soil respiration in a Chinese mountain area. *Agric. For. Meteorol.* **2008**, *148*, 490–503. [[CrossRef](#)]
51. Granier, A.; Ceschia, E.; Damesin, C.; Dufrene, E.; Epron, D.; Gross, P.; Lebaube, S.; Le Dantec, V.; Le Goff, N.; Lemoine, D.; et al. The carbon balance of a young Beech forest. *Funct. Ecol.* **2000**, *14*, 312–325. [[CrossRef](#)]
52. Simmons, J.A.; Fernandez, I.J.; Briggs, R.D.; Delaney, M.T. Forest floor carbon pools and fluxes along a regional climate gradient in Maine, USA. *For. Ecol. Manag.* **1996**, *84*, 81–95. [[CrossRef](#)]
53. Yuji, K.; Mayuko, J.; Masako, D.; Yoshiaki, G.; Koji, T.; Takafumi, M.; Yoichi, K.; Shinji, K.; Motonori, O.; Noriko, M.; et al. Biometric and eddy-covariance-based estimates of carbon balance for a warm-temperate mixed forest in Japan. *Agric. For. Meteorol.* **2008**, *148*, 723–737.
54. Wang, M.; Liu, Y.Q.; Hao, Z.Q.; Wang, Y.S. Respiration rate of broad-leaved Korean pine forest ecosystem in Changbai Mountain. *Chin. J. Appl. Ecol.* **2006**, *17*, 1789–1795. (In Chinese, with English Abstract)
55. Tan, Z.H.; Zhang, Y.P.; Yu, G.R.; Sha, L.Q.; Tang, J.W.; Deng, X.B.; Song, Q.H. Carbon balance of a primary tropical seasonal rain forest. *J. Geophys. Res.* **2010**, *115*, 411–454. [[CrossRef](#)]
56. Law, B.E.; Thornton, P.E.; Irvine, J.; Anthoni, P.M.; Van Tuyl, S. Carbon storage and fluxes in ponderosa pine forests at different developmental stages. *Glob. Chang. Biol.* **2001**, *7*, 755–777. [[CrossRef](#)]
57. Amthor, J.S. Higher plant respiration and its relationships to photosynthesis. *Ecophysiol. Photosynth.* **1993**, *100*, 71–102.
58. Wang, M.; Ji, L.Z.; Li, Q.R.; Xiao, D.M.; Liu, H.L. Stem respiration of *Pinus koraiensis* in Changbai Mountain. *Chin. J. Appl. Ecol.* **2005**, *16*, 7–13. (In Chinese, with English Abstract)
59. Ryan, M.G.; Gower, S.T.; Hubbard, R.M.; Waring, R.H.; Gholz, H.L.; Cropper, W.P., Jr.; Running, S.W. Woody tissue maintenance respiration of four conifers in contrasting climates. *Oecologia* **1995**, *101*, 133–140. [[CrossRef](#)] [[PubMed](#)]
60. Ma, Y.E.; Xiang, W.H.; Lei, P.F. Stem respiration and its controlling factors in forest ecosystems. *Chin. J. Plant Ecol.* **2007**, *31*, 403–412. (In Chinese, with English Abstract)
61. Gough, C.M.; Vogel, C.S.; Kazanski, C.; Nagel, L.; Flower, C.E.; Curtis, P.S. Coarse woody debris and the carbon balance of a north temperate forest. *For. Ecol. Manag.* **2007**, *244*, 60–67. [[CrossRef](#)]
62. Bond-Lamberty, B.; Wang, C.; Gower, S.T. Annual carbon flux from woody debris for a boreal black spruce fire chronosequence. *J. Geophys. Res.* **2002**, *108*, 8220–8230. [[CrossRef](#)]
63. Manies, K.L.; Harden, J.W.; Bond-Lamberty, B.; O'Neill, K.P. Woody debris along an upland chronosequence in boreal Manitoba and its impact on long-term carbon storage. *Can. J. For. Res.* **2005**, *35*, 472–482. [[CrossRef](#)]
64. Progar, R.A.; Schowalter, T.D.; Freitag, C.M.; Morrell, J.J. Respiration from coarse woody debris as affected by moisture and saprotroph functional diversity in Western Oregon. *Oecologia* **2000**, *124*, 426–431. [[CrossRef](#)] [[PubMed](#)]
65. Wang, C.K.; Bond-Lamberty, B.; Gower, S.T. Environmental controls on carbon dioxide flux from black spruce coarse woody debris. *Oecologia* **2002**, *132*, 374–381. [[CrossRef](#)] [[PubMed](#)]
66. Wu, J.B.; Guan, D.X.; Han, S.J.; Pei, T.F.; Shi, T.T.; Zhang, M. Respiration of fallen trees of *Pinus koraiensis* and *Tilia amurensis* in Changbai Mountain, northeastern China. *J. Beijing For. Univ.* **2008**, *30*, 14–19. (In Chinese, with English Abstract)

67. Zhang, S.B.; Zheng, Z.A. Preliminary research on respiration of woody debris of hollow-bearing tree in the montane moist evergreen broad-leaved forest of Ailao Mountain, Yunnan, China. *J. Mt. Sci. Engl.* **2008**, *26*, 300–307.
68. Weedon, J.T.; Cornwell, W.; Cornelissen, J.H.C.; Zanne, A.E.; Wirth, C.; Coomes, D.A. Global meta-analysis of wood decomposition rates, a role for trait variation among tree species? *Ecol. Lett.* **2009**, *12*, 45–56. [[CrossRef](#)] [[PubMed](#)]
69. Shorohova, E.; Ekaterina, K. Influence of the substrate and ecosystem attributes on the decomposition rates of coarse woody debris in European boreal forests. *For. Ecol. Manag.* **2014**, *315*, 173–184. [[CrossRef](#)]
70. Rice, A.H.; Pyle, E.H.; Saleska, S.; Hutyra, L.; Palace, M.; Keller, M.; De Camargo, P.B.; Portilho, K.; Marques, D.F.; Wofsy, S.C. Carbon balance and vegetation dynamics in an old growth Amazonian forest. *Ecol. Appl.* **2004**, *14*, 55–71. [[CrossRef](#)]
71. Cook, B.D.; Bolstad, P.V.; Martin, J.G.; Heinsch, F.A.; Davis, K.J.; Wang, W.G.; Desai, A.R.; Teclaw, R.M. Using light-use and production efficiency models to predict photosynthesis and net carbon exchange during forest canopy disturbance. *Ecosystems* **2008**, *11*, 26–44. [[CrossRef](#)]
72. Nagy, Z.; Pintér, K.; Pavelka, M.; Darenová, E.; Balogh, J. Carbon fluxes of surfaces vs. ecosystems: Advantages of measuring eddy covariance and soil respiration simultaneously in dry grassland ecosystems. *Biogeosciences* **2011**, *8*, 2523–2534. [[CrossRef](#)]
73. Goulden, M.L.; Munger, J.W.; Fan, S.M.; Daube, B.C.; Wofsy, S.C. Measurements of carbon sequestration by long-term Eddy covariance: Methods and a critical evaluation of accuracy. *Glob. Chang. Biol.* **1996**, *2*, 169–182. [[CrossRef](#)]
74. Goulden, M.L.; Wofsy, S.C.; Harden, J.W.; Trumbore, S.E.; Crill, P.; Gower, S.T.; Fries, T.; Daube, B.C.; Fan, S.M.; Sutton, D.J.; et al. Sensitivity of boreal forest carbon balance to soil thaw. *Science* **1998**, *279*, 214–217. [[CrossRef](#)] [[PubMed](#)]
75. Grace, J.; Malhi, Y.; Lloyd, J.; Mcintyre, J.; Miranda, A.C.; Meir, P.; Miranda, H.S. The use of eddy covariance to infer the net carbon dioxide uptake of Brazilian rain forest. *Glob. Chang. Biol.* **1996**, *2*, 209–217. [[CrossRef](#)]
76. Riederer, M.; Serafimovich, A.; Foken, T. Net ecosystem CO₂ exchange measurements by the closed chamber method and the eddy covariance technique and their dependence on atmospheric conditions. *Atmos. Meas. Tech.* **2014**, *7*, 1057–1064. [[CrossRef](#)]
77. Curtis, P.S.; Hanson, P.J.; Bolstad, P.; Barford, C.; Randolph, J.C.; Schmid, H.P.; Wilson, K.B. Biometric and eddy-covariance based estimates of annual carbon storage in five eastern north american deciduous forests. *Agric. For. Meteorol.* **2002**, *113*, 3–19. [[CrossRef](#)]
78. Campioli, M.; Malhi, Y.; Vicca, S.; Luyssaert, S.; Papale, D.; Peñuelas, J.; Reichstein, M.; Migliavacca, M.; Arain, M.A.; Janssens, I.A. Evaluating the convergence between eddy-covariance and biometric methods for assessing carbon budgets of forests. *Nat. Commun.* **2016**, *7*, 13717. [[CrossRef](#)] [[PubMed](#)]
79. Ehman, J.L.; Schmid, H.P.; Grimmond, C.S.B.; Randolph, J.C.; Hanson, P.J.; Wayson, C.A.; Copley, F.D. An initial intercomparison of micrometeorological and ecological inventory estimates of carbon exchange in a mid-latitude deciduous forest. *Glob. Chang. Biol.* **2002**, *8*, 575–589. [[CrossRef](#)]
80. Clark, D.A.; Brown, S.; Kicklighter, D.W.; Chambers, J.Q.; Thomlinson, J.R.; Ni, J. Measuring net primary production in forests: Concepts and field methods. *Ecol. Appl.* **2001**, *11*, 356–370. [[CrossRef](#)]
81. Houghton, R.A.; Skole, D.L.; Nobre, C.A.; Hackler, J.L.; Lawrence, K.T.; Chomentowski, W.H. Annual fluxes of carbon from deforestation and regrowth in the Brazilian Amazon. *Nature* **2000**, *403*, 301–304. [[CrossRef](#)] [[PubMed](#)]
82. Fang, J.Y.; Chen, A.P.; Peng, C.H.; Zhao, S.Q.; Ci, L.J. Changes in forest biomass carbon storage in China between 1949 and 1998. *Science* **2001**, *292*, 2320–2322. [[CrossRef](#)] [[PubMed](#)]
83. Gough, C.M.; Vogel, C.S.; Schmid, H.P.; Su, H.B.; Curtis, P.S. Multi-year convergence of biometric and meteorological estimates of forest carbon storage. *Agric. For. Meteorol.* **2008**, *148*, 158–170. [[CrossRef](#)]
84. Vicca, S.; Luyssaert, S.; Peñuelas, J.; Campioli, M.; Chapin, F.S.; Ciais, P.; Heinemeyer, A.; Höglberg, P.; Kutsch, W.L.; Law, B.E.; et al. Fertile forests produce biomass more efficiently. *Ecol. Lett.* **2012**, *15*, 520–526. [[CrossRef](#)] [[PubMed](#)]

